

PAPER • OPEN ACCESS

## Wavy plates as impinging oil separating structure at compressor discharge

To cite this article: Jiu Xu and Pega Hrnjak 2019 *IOP Conf. Ser.: Mater. Sci. Eng.* **604** 012031

View the [article online](#) for updates and enhancements.

# Wavy plates as impinging oil separating structure at compressor discharge

Jiu Xu<sup>1</sup>, Pega Hrnjak<sup>1,2,\*</sup>

<sup>1</sup> University of Illinois at Urbana-Champaign, Mechanical Science and Engineering, Urbana, IL, USA

<sup>2</sup> CTS, Creative Thermal Solutions, Urbana, IL, USA

pega@illinois.edu

**Abstract.** Oil separation is commonly needed in air conditioning and refrigeration systems to reduce the oil circulation rate and keep the oil inside the compressor. For compactness, the oil separation structure integrated into the compressor is more and more popular than traditional external oil separators. This paper presents the impinging separation mechanism, one of the basic mechanisms of droplet separation. As a representative of the impinging separator, wave-plates structures are studied by flow visualization and experimental measurement under realistic compressor discharge conditions. The video of oil mist flowing through the baffles and plates is captured by a high-speed camera and analyzed quantitatively. The effect of the oil flow condition and the effect of separator geometry design are investigated based on the experimental data. With the help of flow visualization, the flow details are analyzed.

## 1. Introduction

Oil provides lubrication to the moving parts in the compressor, helps to seal the gap between parts and removes heat generated from the vapor compression. Though essential in compressors, oil circulating in other system components, like condenser and evaporator, brings adverse effects. It may build up as a thin oil film on the internal surfaces of heat exchangers reducing the heat transfer and adds the pressure drop. Therefore, for vastly dominant *lubricated* compressors, oil management is a key issue to ensure the reliability and efficiency of the system. Oil separators serve to regulate and minimize oil circulation by separating the lubricant early at the compressor discharge port and return it to the compressor.

Oil separators are commonly used in refrigeration or air conditioning systems to reduce the oil circulation ratio (OCR). OCR is a parameter to quantify the amount of oil circulating in the system. It is defined as the mass flow rate of oil divided by the total mass flow rate of the refrigerant-oil mixture in the system. The ideal goal is to remove all the oil from the refrigerant-oil mixture at compressor discharge so that no oil escapes from the compressor and it has no effect on heat transfer or pressure drop. In reality, the oil separator has a certain separation efficiency (below 100%), and it introduces extra pressure drop and volume.

Typically, the oil separator is installed between the compressor discharge and condenser inlet, where the refrigerant is in the vapor phase. The separation structure captures the oil mist, and the oil drains down to the bottom of the separator due to gravity. The volume of the oil separator can hold some oil temporarily. The oil will return to the crankcase of the compressor when it reaches a certain level. For compact systems, it is more common to integrate some oil separation structure into the extended volume of the compressor.



The characteristics of oil flow at the compressor discharge are the pre-requisite information for oil separator designs. Many researchers have developed methods to quantify the oil ejecting by the compressor, especially the oil mist and oil film at the compressor discharge [1]–[5]. It is observed that the oil droplets are formed by oil film breakup due to the periodic reed valve movement. The oil droplets are then entrained by the refrigerant vapor and leave the compressor to form a mist-annular developing flow in the discharge pipe. The oil mist characteristics, including oil droplet size distribution and oil droplet velocity distribution, are affected by compressor working condition, compressor internal geometry, and oil properties.

The oil separator design relies on the understanding of the basic mechanisms of mist elimination. Impingement is one of the basic mechanisms for droplet separation. The fundamental principle of separation is the capture of droplets by the surface of baffles or vanes. The liquid film is formed after the capture of the droplets and drain down to the bottom due to the gravity. Many different geometries have been applied to separate the droplets from the vapor flow in different engineering processes.

Impinging oil separators have been successfully applied in the compressors in the refrigeration industry for decades, but some fundamental questions remain unanswered. This chapter focuses on the impinging oil separator for refrigerant compressors. Wave-plates are studied as a representative design of impinging separators. Flow visualization technique is carried out to characterize the oil flow details through the separation structure. Separation efficiency and pressure drop are measured experimentally and simulated numerically to evaluate the performance of different separation structures. The analysis of some typical imping separator aims to provide design guidelines for structure based on impinging separation mechanism.

## 2. Methods

### 2.1. Experimental Setup

An air conditioning test bench is built for this study to quantify the performance of the oil separation structure and capture the video of refrigerant-oil mixture simultaneously (Figure 1). A swashplate reciprocating compressor works as the source of oil mist flowing into the oil separator. The swashplate reciprocating compressor is selected because it is easy to control the OCR in a relatively large OCR range. The speed of the compressor is controlled by a motor and a variable frequency driver. The refrigerant-oil mixture leaving the compressor enters the visualization chamber. Part of the oil is separated and accumulates to form a steady oil level in the draining pipe. The flow visualization is realized by putting a transparent visualization chamber between the compressor outlet and the condenser inlet. Separation structure of various geometries is installed into the chamber for the test. The visualization chamber is served as the container while the separation structure is the filler.

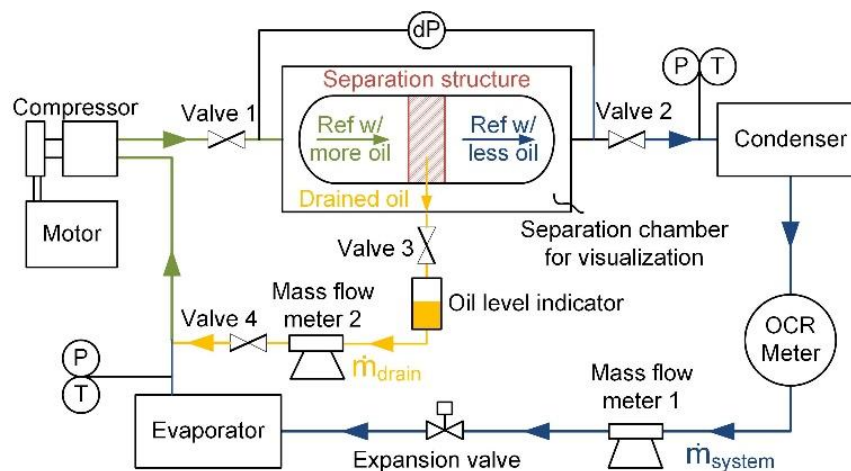


Figure 1. Experimental facilities of the oil separation study

Valve 3 and 4 (shown in Figure 1) control the flow of collected oil from the bottom of the chamber to the suction of the compressor. The mass flow rate ( $\dot{m}_{\text{drain}}$ ) of the returned oil is measured by a Coriolis type mass flow meter 2. Valve 4 is adjusted to ensure that only single-phase oil pass the mass flow meter and the oil level is steady in the system steady state. The steady oil level indicates there is no accumulation or over-draining in the oil level indicator, so  $\dot{m}_{\text{drain}}$  can reflect the actual draining rate. Refrigerant and the carry-over oil flows through the condenser, expansion valve, evaporator, and finally returns to the compressor.

In the liquid line between the condenser and the expansion valve, the mass flow rate of the system ( $\dot{m}_{\text{system}}$ ) is measured by another Coriolis type mass flow meter, and the OCR is measured by a speed-of-sound type oil concentration meter. The oil concentration meter is calibrated by comparing the meter reading with the result using traditional sampling method [6], [7].

The separation efficiency is the most important parameter of an oil separator. In this experimental setup, two separation efficiencies are measured: overall separation efficiency and structure separation efficiency. The overall separation efficiency is defined as the mass flow rate of the actually-separated oil by the whole oil separator divided by the mass flow rate of the oil coming to the oil separator. The overall separation efficiency considers the separation caused by the chamber and the separation structure together. With the measurement of  $\dot{m}_{\text{drain}}$  and  $\dot{m}_{\text{system}}$ , the overall separation efficiency can be calculated by equation (1). Here,  $\omega$  is the solubility of refrigerant in the refrigerant-oil mixture, determined by the property correlations by [8]. OCR is the oil circulation ratio measured by the OCR meter in the liquid line.

$$\eta_o = \frac{\dot{m}_{\text{drain,oil}}}{\dot{m}_{\text{in,oil}}} = \frac{\dot{m}_{\text{drain}}(1 - \omega)}{\dot{m}_{\text{drain}}(1 - \omega) + \dot{m}_{\text{system}} \cdot \text{OCR}} \quad (1)$$

Compared to the overall separation efficiency, structural separation efficiency is more favorable when we want to compare different separation structures in a specific volume. The structure separation efficiency excludes the effect of the container volume and focuses only on the separation structure itself. It is defined as the mass flow rate of drained oil by the separation structures divided by the total mass flow of oil droplets going to the separation structure. In this experimental setup, it is determined by comparing the video taken before and after the filler. The mass flow rate of oil mist before and after the filler is estimated by the sampling video taken before and after the filler. The video locations are shown in Figure 3. In this way, the filler separation efficiency is calculated by equation (2). Here the subscript “bs” refers to “before structure” while the subscript “as” refers to “after structure”.

$$\eta_s = \frac{\dot{m}_{\text{bs,oil}} - \dot{m}_{\text{as,oil}}}{\dot{m}_{\text{bs,oil}}} \quad (2)$$

Pressure drop is another important measure of performance of the oil separator. A differential pressure transducer is installed to measure the pressure drop across the separation structure. The high-side and low side of the differential pressure transducer are connected to the inlet and the outlet of the separation chamber for visualization, respectively.

The uncertainty of the measurement mainly comes from the uncertainty of the instrument. For the separation efficiency, the uncertainty of the mass flow meter is  $\pm 0.35\%$  of the reading. For the pressure drop, the uncertainty of the differential pressure transmitter is  $\pm 0.25\%$  of the span, about 0.09 kPa. The error bar shown in Figure 5 and Figure 7 is calculated by the uncertainty propagation.

## 2.2. Manufacture and geometry of the separating structure

The separation structure is fabricated by stereolithography apparatus (SLA). The material is WaterClear Ultra 10122, an optically clear resin with ABS-like properties and good temperature resistance. It produces colorless, functional, accurate parts that simulate acrylic in appearance as shown in Figure 2.

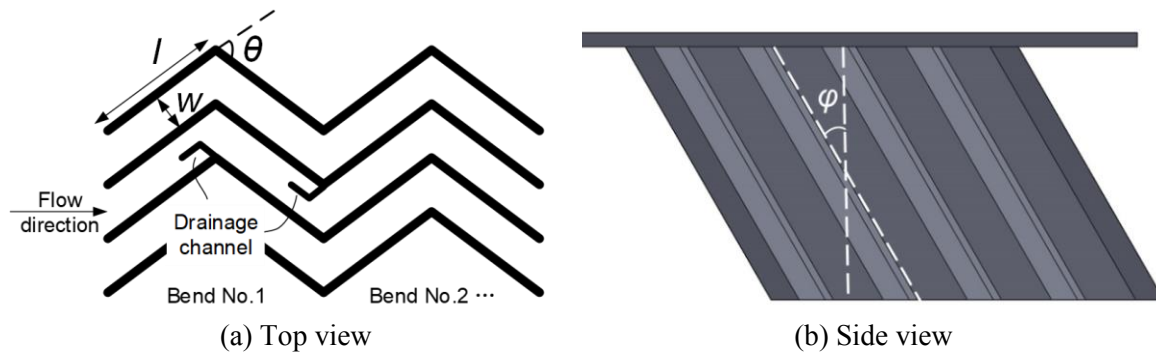


Figure 2. Visualization chamber for oil separator tests (a) structure of the chamber; (b) location where the video is captured

The plate length  $l$  is the length of a straight plate along the flow direction. The gap width  $w$  defines the distance between two zigzag plates. The stage number is the number of bends along the flow direction. The bend angle  $\theta$  is the angle between two neighboring plates, which reflects the change of flow direction. The inclination angle  $\phi$  is the angle between the flow direction and the waveplate. In this study, the effect of gap width, stage number, drainage channel, and inclination angle are investigated by comparing the separation efficiency and the pressure drop of different geometries. The details of the wave plates used in our tests are listed in Table 1. There are eight geometries that were evaluated:

- 1) *Benchmark* (BM) geometry is firstly fabricated to be the reference for other geometries.
- 2) Reduced gap (“w-” means a wave-plates with smaller gap width than 3.21 for benchmark but all the other geometric specifications are the same)
  - a) Gap width = 2.06 mm
  - b) Gap width = 1.6 mm
- 3) Additional bends (“n+” represents the variation of the number of bends compared to 4 in BM).
  - a) Number of bends = 6
  - b) Number of bends = 2
- 4) Added drainage channel (“DC” means the drainage channels are added to the original geometry).
- 5) Inclined bends and drainage channel (“ $\phi$ +” represents the increasing inclination angle).
  - a) Inclination angle =  $15^\circ$
  - b) Inclination angle =  $30^\circ$
  - c)

Table 1: Geometry details of the tested wave plates

| Name        | Gap width<br>$w$ [mm] | Number of<br>bends $n$ | Inclination<br>angle $\phi$ [ $^\circ$ ] | Bend angle<br>$\theta$ [ $^\circ$ ] | Plate length $l$<br>[mm] | Plate height<br>$h$ [mm] | Drainage<br>channel? |
|-------------|-----------------------|------------------------|--|-------------------------------------|--------------------------|--------------------------|----------------------|
| BM          | 3.21                  | 4                      | 0  | 80                                  | 7.59                     | 38                       | N                    |
| w-          | 2.06                  | 4                      | 0  | 80                                  | 7.59                     | 38                       | N                    |
| w--         | 1.6                   | 4                      | 0  | 80                                  | 7.59                     | 38                       | N                    |
| w-n+        | 2.06                  | 6                      | 0  | 80                                  | 7.59                     | 38                       | N                    |
| w-n-        | 2.06                  | 2                      | 0  | 80                                  | 7.59                     | 38                       | N                    |
| DC          | 3.21                  | 4                      | 0  | 80                                  | 7.59                     | 38                       | Y                    |
| $\phi$ +DC  | 3.21                  | 4                      | 15                                       | 80                                  | 7.59                     | 38                       | Y                    |
| $\phi$ ++DC | 3.21                  | 4                      | 30                                       | 80                                  | 7.59                     | 38                       | Y                    |

### 2.3. Flow visualization and video processing

The test section presented in Figure 3. is built by attaching transparent windows to an aluminum frame. One inlet hole and one outlet hole are in the direction of flow while another hole for draining oil is located at the bottom of the frame. Two smaller holes on the top of the block are reserved for connections of the differential pressure transducer. O-rings and gaskets are used to seal the test section and hold the pressure at the compressor discharge. The visualization chamber is designed to provide

relatively uniform incoming vapor flow on the cross-sectional area. The design of the test section makes oil mist flow visible, but the disadvantage is that the geometry slightly differs from the typical.

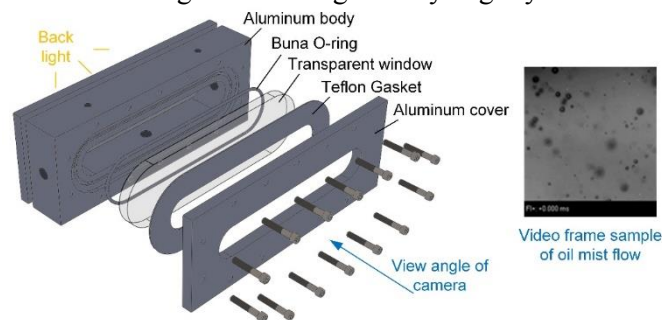


Figure 3. Visualization chamber for oil separator tests (a) structure of the chamber; (b) location where the video is captured

The backlight provides high contrast between the bright background and dark image of the droplets so that the camera can capture the clear video of the oil mist and the details of the separation. Videos of oil mist are taken before and after the separation structure at the steady state. The locations of the video captures are shown in Figure 3 and marked as “video frames”. These videos are then processed to estimate the droplet size distribution and oil volume fraction of the oil mist. Qualitative videos of flow details in the separation structure are also captured to provide a general image of the interaction between the oil droplets and the separation structure. A set of video processing techniques were developed to quantify the videos of the oil mist by [3]. Processed videos of the oil mist before and after the separation structure provide droplet size and velocity distribution as well as liquid volume fraction.

In this study, only videos of oil mist before and after the separation structure are processed to get the droplet size distribution and liquid volume fraction of a cluster of oil droplets. By processing the video of the oil mist before and after the separator, droplet size distribution, droplet velocity distribution and liquid volume fraction are obtained for further analysis.

### 3. Effect of flow conditions

#### 3.1. Test conditions

The experiments were carried out to study both the effect of flow condition and the effect of geometric design on the performance of the impinging separators. Each separating structure is tested under the same group of working conditions. For different working conditions, the system mass flow rate changes while the compressor discharge pressure and temperature are maintained at the same by adjusting the condensing and evaporating capacity. All the measurements are made at steady state. In the transition between steady states, the refrigerant and oil mixture flow in the bypass line. At the steady state, the flow goes through the visualization chamber, and the flow details are captured by the high-speed camera. The test condition details are shown in Table 2.

Table 2: General test conditions

|                                  | Value                    |
|----------------------------------|--------------------------|
| Type of refrigerant              | R134a                    |
| Type of oil                      | PAG 46                   |
| Type of compressor               | Swashplate reciprocating |
| With oil sump?                   | No                       |
| Compressor speed                 | 1800 RPM                 |
| Mass flow rate                   | 6 ~ 20 g/s               |
| OCR before separator             | 2 ~ 10%                  |
| OCR after separator              | 0.5~ 1.5%                |
| Compressor discharge pressure    | 750 kPa                  |
| Compressor discharge temperature | 80 °C                    |



### 3.2. Refrigerant vapor flow condition

The performance of a separating structure is influenced by the vapor flow condition and the characteristics of the oil mist. The actual flow field and the corresponding oil droplet distribution through the wave plates can be very complex, so we simplify the discussion by focusing on the overall vapor flow velocity.

For the refrigerant vapor, vapor superficial velocity is used to represent how fast the refrigerant-oil mixture passes the separation structure. Vapor superficial velocity is defined as the volumetric flow rate of the refrigerant-oil mixture in the test section divided by the cross-sectional area of the test section, as shown in equation (3). The reason to use vapor superficial velocity instead of mass flow rate as the primary variable is that the mass flow rate is strongly affected by the system working condition and compressor type. Conclusions based on vapor superficial velocity are more generalizable so that they can be applied in oil separation for different compressors and fluids. In the plots below, the mass flow rate of the system is also plotted in the secondary horizontal axis as a reference.

$$u_{vs} = \frac{\dot{m}_{\text{system}}(1 - \text{OCR})}{\rho_v A} \quad (3)$$

### 3.3. Oil mist characteristics

Upstream oil flow condition has a significant impact on the separation efficiency and pressure drop of the impinging oil separators. In this paper, we use vapor superficial velocity to distinguish different flow conditions. The system mass flow rate is also plotted as the secondary variable.

The droplet size distribution provided by the video processing is also shown in Figure 4. The droplet diameter of the oil mist follows the log-normal distribution. It is not surprising to see the total mass flow rate contributed by the oil mist decreases after the oil mist passes through the wave-plates. Also, the mean droplet diameter becomes smaller when the oil mist passes through the wave-plates, which indicates that bigger oil droplets are easier to be separated.

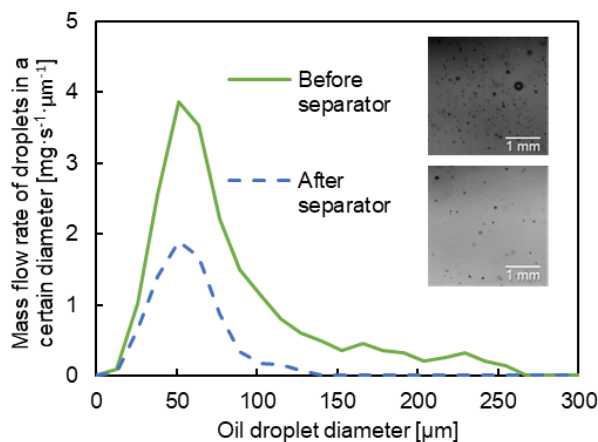


Figure 4. Droplet size distribution before/after the 'BM' impinging structure (geometric specification listed in Table 1) at vapor superficial velocity of 0.27 m/s

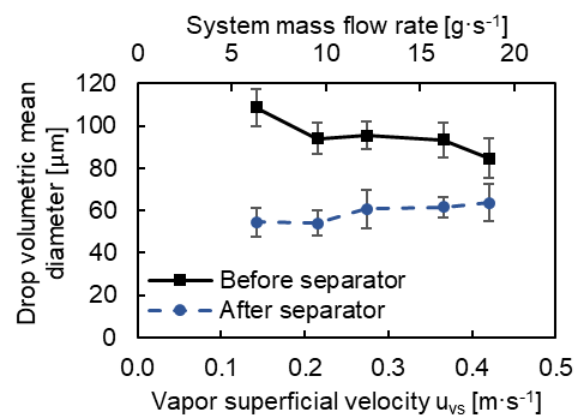


Figure 5. The effect of the incoming flow condition on the oil droplet mean diameter of the 'BM' impinging structure (geometric specification listed in Table 1)

Though the droplet size distribution can explicitly describe the oil mist before or after the separator, it contains too much information for a simple comparison between one operating condition with another. We can use the oil droplet volumetric mean diameter as a more concentrated parameter to represent the oil mist characteristics at one particular flow condition. There are many ways to calculate the mean diameter of a group of oil droplets. Here we use the volume mean diameter. The volumetric mean diameter is a representative description of the size of the oil droplets considering the droplet volume.

Figure 5 shows the effect of system flow rate (vapor superficial velocity) on the oil droplet mean diameter before and after the separator. In general, droplet mean diameter at the discharge of the compressor (before the separator) decreases as the vapor superficial velocity increases. The volumetric

mean diameter of the oil droplets after the separator is smaller than that before the separator, which is also reflected in the distribution in Figure 4. The sampling video after the separator captured the escaped small oil droplets.

Besides the vapor phase superficial velocity and oil droplet size, oil mass flow rate may also affect the performance of the impinging oil separators. Oil mass flow rate is positively related to the system mass flow rate or vapor superficial velocity in the separator chamber. Figure 6 shows the oil mass flow rate through the benchmark impinging oil separator as a function of the vapor superficial velocity. The oil mass flow rate entering the separation chamber increases as the vapor velocity increases. The majority of the oil coming into the separator is separated and drained back to the compressor suction, and the rest is carried over by the refrigerant vapor. The ratio of the drained oil and the total incoming is the separation efficiency. It indicates that separation efficiency decreases as the vapor velocity increases though the amount of separated oil slightly increases.

To summarize, the refrigerant-oil mixture entering the oil separator shows the following trends as the system mass flow rate getting higher. 1) Refrigerant vapor superficial velocity rises; 2) Mass flow rate of oil rises; 3) Number of oil droplets in a specific volume for a certain period of time increases; 4) Oil droplet volumetric diameter decreases.

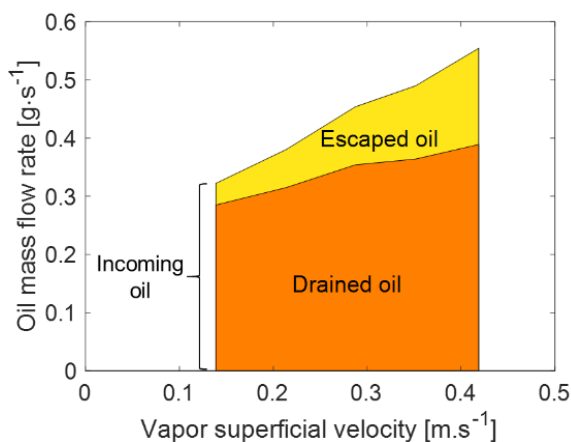


Figure 6. The effect of the incoming flow condition on the oil mass flow rate of the 'BM' impinging structure (geometric specification listed in Table 1)

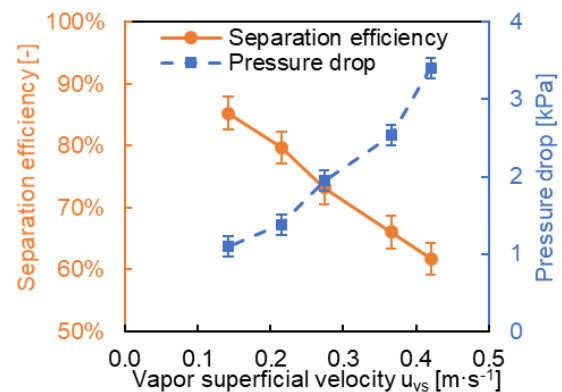


Figure 7: Separation efficiency and pressure drop of the 'BM' impinging structure (geometric specification listed in Table 1) under varying working conditions

### 3.4. Separation efficiency and pressure drop

Separation efficiency is the most important parameter of the oil separation structure. Figure 7 plots the separation efficiency and the corresponding pressure drop of the benchmark geometry as a function of vapor superficial velocity. The separation efficiency drops as the vapor superficial velocity increases. Higher vapor superficial velocity also means higher system mass flow rate, higher upstream oil mass flow rate and smaller droplet mean diameter. Therefore, the trend of separation efficiency as a function of vapor superficial velocity can be explained by two aspects. First, a larger amount of finer oil droplets is more difficult for the separator in general. Small oil droplets are able to follow the vapor flow without hitting the surface of the baffles. Second, refrigerant vapor with higher velocity may entrain the captured oil and increases the possibility of the oil droplet reflection by the surface.

The pressure drop is one of the main performance cost of introducing an oil separator, besides extra volume and components to the system. When comparing the same separator at different flow conditions, the pressure drop increases as the velocity of the vapor phase increases. By linking separation efficiency with pressure drop, it can be concluded that a separator with higher separation efficiency usually cost more pressure drop. This indicates a trade-off between separation efficiency and pressure drop for the design of oil separators.



## 4. Effect of geometric design

### 4.1. Gap width

Upstream oil flow condition has a significant impact on the performance of an impinging oil separator. In practice, the upstream flow condition is determined by the compressor working condition, and we can only change the geometry design of the oil separator to fit this condition.

The effect of the gap width can be seen by comparing the results of geometry 'BM', 'w-' and 'w--', as shown in Figure 8(a)(b). Reducing the gap width between the plates means that more channels and more surface area can be fitted in a certain volume. Therefore, the impinging separator with a smaller gap width achieves higher separation efficiency and introduces a larger pressure drop, as shown in the trend in Figure 8(c).

### 4.2. Number of bends

The effect of the number of bends can be seen by comparing the results of geometry 'w-', 'w-n-' and 'w-n+'. More bends along the flow direction mean higher chance that oil droplets are captured. As a result, wave-plates with larger bend number has higher separation efficiency (shown in Figure 9). From the observation of the flow visualization results, it can be concluded that more oil droplets are captured in the bend closer to the oil flow inlet. More bends along the flow direction mean higher chance that oil droplets are captured. As a result, wave-plates with larger bend number has higher separation efficiency. More bends also mean more friction between the vapor phase and the solid phase, so more bends introduce higher pressure drop (shown in Figure 9).

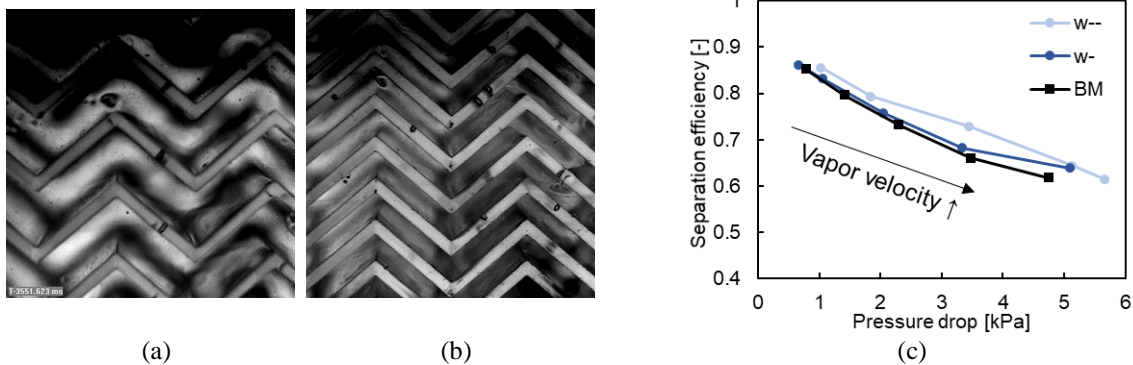


Figure 8. Oil mist through two wave-plates with different gap width (top view): (a) separator 'BM'; (b) separator 'w--'; (c) separation efficiency and pressure drop of 'BM', 'w-', 'w--'

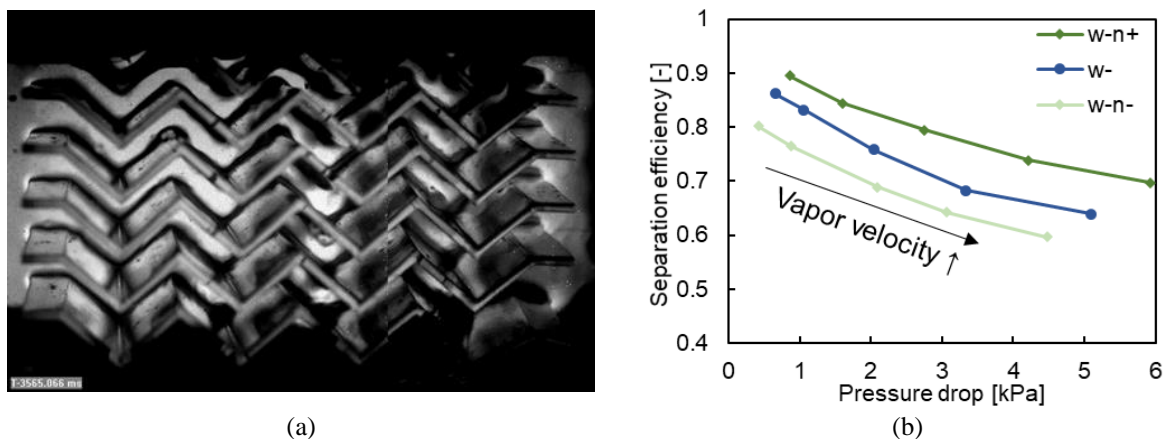


Figure 9. Oil mist through wave-plates with 7 bends (top view): (a) separator 'w-'; (c) separation efficiency and pressure drop of 'w-n+', 'w-', 'w-n-'

#### 4.3. Effect of drainage channels

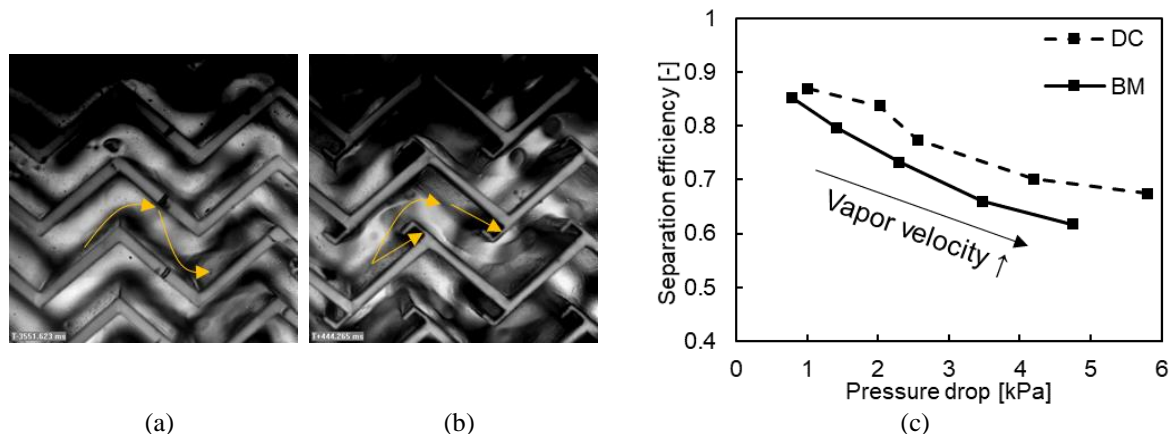


Figure 10. Oil mist through two wave-plates with different gap width (top view): (a) separator 'BM'; (b) separator 'DC'; (c) separation efficiency and pressure drop of 'BM' and 'DC'

The effect of drainage channel can be seen by comparing the results of geometry 'BM' and 'dc'. In the separation of oil mist, deposited oil is collected at the bend corners and may be re-entrained into the stream of refrigerant vapor. This leads to a reduction in separation efficiency, as shown in Figure 10. To prevent re-entrainment, drainage channels are introduced at the bend corners to help the drainage of the captured oil film. Figure 10(a)(b) show a top view video frame of the oil mist passing through two different wave plates. The visualization shows that the hook of the drainage channel can retain some of the oil and prevent the entrainment. Therefore, the separation efficiency of the structure with drainage channels is higher than that of the structure without drainage channels. The pressure drop also increases when we introduce extra solid surfaces to the original wave-plates.

#### 4.4. Inclination angle

In some cases, the quantity of separated oil at each plane are too high for the drain channel to drain well so oil starts to overflow and be re-entrained. To avoid that to happen, there are two basic options: one is to enlarge the channel which will increase pressure drop and local vapor velocity and the other to incline the structure and add shear and inertial forces to help gravity in providing the mechanism for draining.

The effect of inclination angle can be seen by comparing the results of geometry 'DC', ' $\phi$ +DC' and ' $\phi$ ++DC'. One advantage of inclination angle is that the vapor flow brings a shear force along the drainage direction, as shown in Figure 11(a)(b). The vapor-introduced shear can potentially accelerate the flow of the oil film. However, the drainage distance also increases when the inclining angle exists, if we assume the destination of the draining oil is the bottom of the chamber. As a result, the competence of these two factors mentioned have not shown a strong effect on the separation efficiency and pressure drop (as shown in Figure 11(c)) of the wave plates with different inclination angles.

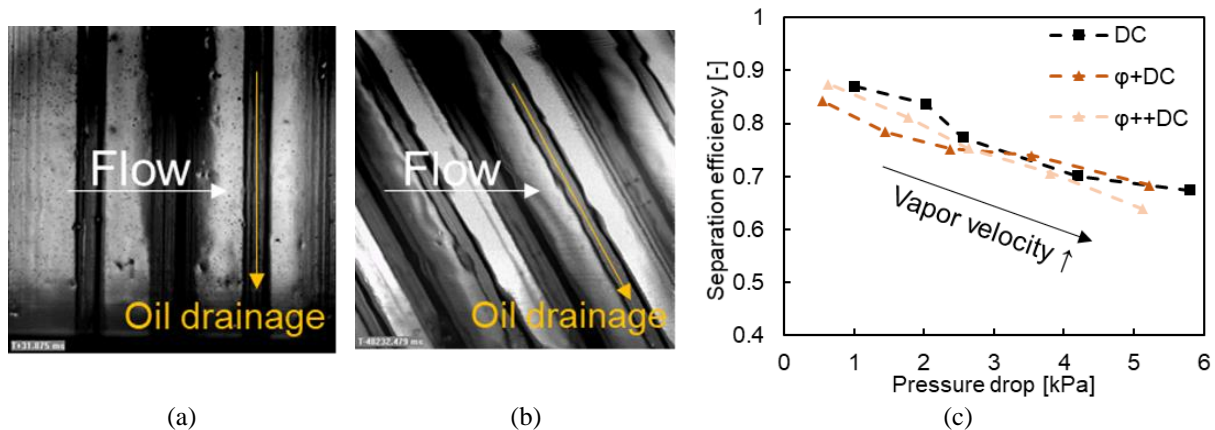


Figure 11. Oil mist through two wave-plates with different gap width (top view): (a) separator 'BM'; (b) separator 'DC'; (c) separation efficiency and pressure drop of 'BM' and 'DC'

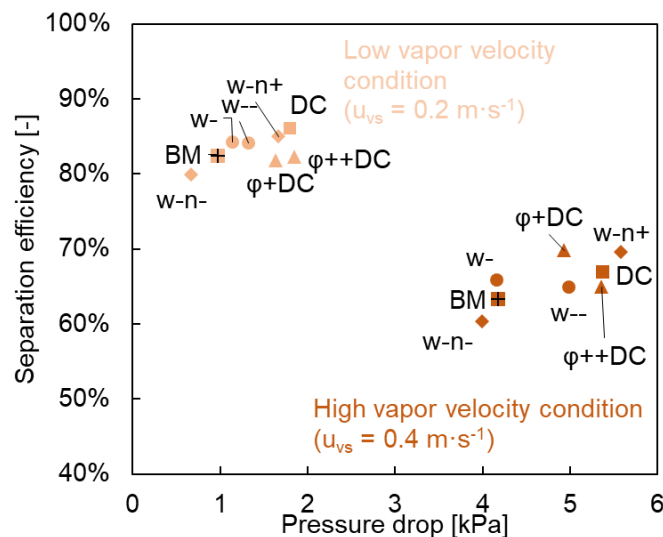


Figure 12. Evaluation of different impinging separator geometries under low or high vapor velocity

#### 4.5. Design suggestions

The separation efficiency and pressure drop of all eight different wave-plates design at two flow conditions (low vapor velocity case and high vapor velocity case) are plotted in Figure 12. The data points are extrapolated from the original curve to make sure the comparison between the separator geometries is at the same flow condition. All the wave-plates are tested from low vapor velocity to high vapor velocity condition. In this design map, the upper left corner is the best option, where separation efficiency is high and pressure drop is low. The lower right corner is the opposite.

By comparing the separation efficiency and pressure drop of different geometries, it can be concluded that reducing the gap width, adding more bends and adding drainage channel can increase the separation efficiency but also introduces extra pressure drop. When the vapor superficial velocity gets higher, the overall performance of the impinging oil separator gets worse. The geometry design of the separator should consider both the effect of flow condition and the effect of the separator geometry. Many more different designs can be tested, but more fundamental analysis is needed to guide the design of better impinging oil separators.

### 5. Summary

This paper focuses on the design of the impinging separator, specifically:

- Flow visualization and experimental measurement of the imping oil separator at the realistic compressor discharge conditions are presented and discussed. Besides qualitative insights

quantification includes droplet size distribution and oil volume fraction. The observation of oil mist passing the impinging oil separator also provide good explanation of the effect brought by different flow conditions and different geometries

- Flow condition has a significant impact on the performance of impinging oil separators. Experimental measurement shows that separation efficiency decreases when vapor velocity increases. High kinetic energy of the oil droplets increase the possibility of the reflection of the droplets. Vapor flow with high momentum breaks the oil film on the wire into oil droplets and those oil droplets are entrained by the high-velocity vapor flow. Pressure drop introduced by the separation structure increases as the vapor velocity goes up
- Geometry also affects the performance of impinging oil separators. Furthermore, the geometric specification is the designable variable that can be tuned toward optimization when the compressor discharge flow condition is typically given in practices. The experiments show that reducing gap width, adding bend number and adding drainage channels can increase the separation efficiency but at the cost of higher pressure drop.

### Acknowledgements

The authors would like to acknowledge the support of the member companies of the Air Conditioning and Refrigeration Center at the University of Illinois at Urbana-Champaign. The authors would also like to acknowledge the significant contributions made by Dr. Scott Wujek, Dr. Augusto Zimmermann in while they were PhD students, Dr. Ye Feng and Mr. Junqi Ma.

### References

- [1] S. Wujek and P. Hrnjak, "Mist to annular flow development quantified by novel video analysis. ACRC Report TR285," Urbana, 2011.
- [2] A. Zimmermann and P. Hrnjak, "Oil flow at discharge valve in a scroll compressor.," Proc. Inst. Mech. Eng. Part E J. Process Mech. Eng., vol. 229, no. 2, pp. 104–113, 2015.
- [3] A. Zimmermann, "Experimental investigation of mist flow generated by reed valves in compressor discharge," University of Illinois at Urbana-Champaign, 2016.
- [4] J. Xu and P. Hrnjak, "Quantification of flow and retention of oil in compressor discharge pipe," Int. J. Refrig., vol. 80, 2017.
- [5] J. Xu and P. Hrnjak, "Formation, distribution, and movement of oil droplets in the compressor plenum," Int. J. Refrig., vol. 93, pp. 184–194, Sep. 2018.
- [6] ASHRAE, "ASHRAE Standard 41.4: Method for measurement of proportion of lubricant in liquid refrigerant," Tech. Report, ASHRAE, vol. 1996, no. Ra, 2006.
- [7] J. Xu and P. Hrnjak, "Refrigerant-Oil Flow at the Compressor Discharge," in SAE Technical Paper 2016-01-0247, 2016.
- [8] C. Seeton and P. Hrnjak, "CO<sub>2</sub>-Lubricant Two-Phase Flow Patterns in Small Horizontal Wetted Wall Channels: The Effects of Refrigerant/Lubricant Thermophysical Properties," Urbana, 2009.